The Effects of Composite Plate Design Parameters on Linear Vibrations by Discrete Singular Convolution Method

ABDULLAH SEÇGIN,* CESIM ATAS AND A. SAIDE SARIGÜL
Dokuz Eylül University, Department of Mechanical Engineering
35100, Bornova, İzmir, Turkey

ABSTRACT: This study is devoted to some specific free vibration analysis of thin composite plates based on discrete singular convolution (DSC) approach. As the first analysis, a parametric study is performed on the basis of number of lamination, boundary condition, and orientation angle of symmetrically laminated composite plates. As the second, the effects of material type, boundary condition, and stacking sequence on the modal characteristics of laminated plates made of E-glass/epoxy, Kevlar/epoxy, and carbon/epoxy are investigated. Thirdly, linear modal characteristics of fiber metal laminates are specifically analyzed due to their common use in aircraft design. Hopefully, the results presented in the article may be practically of interest for engineers and designers. This study displays the applicability of the DSC method for real-life problems.

KEY WORDS: discrete singular convolution, free vibration, thin composite plate, FML.

INTRODUCTION

COMPOSITE PLATES GENERALLY are made of alternating layers of fiber-reinforced polymer prepregs or different combinations of polymer prepregs and metals. The material type and orientation angle of the layers drastically change the modal characteristics of the composites beside the mechanical properties such as strength, roughness, durability, fatigue, and fracture behavior. As it is known, in the dynamic analysis of structures, free vibration analysis has primary importance. Free vibrations of thin plates have been examined by many researchers due to their sensitivity to excitations. Since the application of composite materials to real-life structures, the researches on vibrational characteristics of composite structures, including thin plates, have been accelerated. Among them, some studies include specific numerical applications considering thin composite plates made of three different polymer materials: Leissa and Narita [1] have examined the effects of

*Author to whom correspondence should be addressed. E-mail: abdullah.secgin@deu.edu.tr
Figures 1–9 and 11–14 appear in color online: http://jcm.sagepub.com

0021-9983/09/24 2963–24 $10.00/0 DOI: 10.1177/0021998309345339

material, number of layers, and fiber orientation on the natural frequencies and mode shapes of simply supported plates made of E-glass/epoxy, boron/epoxy, and graphite/epoxy. Chow et al. [2] have made contribution to Leissa and Narita's study by analyses of clamped plates. Hung et al. [3] have extended Chow et al.' work by including the combinations of simply supported, clamped, and free boundary conditions.

Hybrid composites offer superior mechanical properties over conventional composite laminates and high-strength metal alloys. Specifically, fiber metal laminates (FML) combine the good fatigue and fracture behavior of polymer composites with the excellent durability, toughness, and impact resistance of metals in addition to the weight and cost reductions. Due to these excellent properties, FMLs are being used in commercial aircrafts and advanced aerospace structures [4–7]. However, the number of vibration analyses presented for hybrid composites in literature is limited. These studies were generally performed based on geometrical nonlinearity and including initial stresses [8–11].

In this study, a numerical technique, discrete singular convolution (DSC) approach originally introduced by Wei [12–14] was used. The DSC has been successfully used in various free vibration analyses of isotropic thin simple structures with several boundary conditions [15–23]. Hou et al. [24] have used DSC-Ritz method for free vibration analysis of thick plates and shells. Civalek [25–27] has applied DSC approach to free vibration and buckling analyses of different laminated shells and plates. Seçgin et al. [28] have used the DSC for free vibration of fiber–metal laminated composite plates. Seçgin and Sarıgül [29] have performed validation studies for the DSC and showed the superiority of this approach over several numerical techniques for symmetrically laminated thin composite plates. In the present study, it has been intended to apply the DSC to the free vibration analysis of composite plates based on CLPT in order to figure out the modal characteristics affected by the design parameters. Design parameters are material type, stacking sequence, number of plies in each stack, and boundary conditions. Three different studies labeled as Investigation A, B, and C are independently considered for practical purposes. In Investigation A, symmetrically laminated three-ply, four-ply, and five-ply composite plates with six different boundary conditions are considered in order to examine the effects of number of plies and orientation angle on natural frequency parameters. In Investigation B, the effects of material type and stacking sequences on the modal characteristics of laminated plates made of E-glass/epoxy, Kevlar/epoxy, and carbon/epoxy with two different boundary conditions are investigated. In Investigation C, due to their practical importance, FML are specifically considered on a linear base in order to compare the effects of material type of fiber, boundary condition, and orientation angle on natural frequency parameters. The results are evaluated together with those of monolithic aluminium alloys.

DISCRETE SINGULAR CONVOLUTION

DSC Theory

A singular convolution can be given as [12]:

$$F(t) = (T^{*}\eta)(t) = \int_{-\infty}^{\infty} T(t-x)\,\eta(x)\,\mathrm{d}x. \tag{1}$$

Here, T is a distribution, $\eta(t)$ is an element of the space of test functions, the sign * is the convolution operator, $F(t)$ is the convolution of η and T, $T(t-x)$ is the singular kernel of the convolution integral. Delta kernel is commonly used as an interpolation expression for numerical solution of partial differential equations:

$$T(x) = \delta^n(x) \quad n = 0, 1, 2, \ldots \tag{2}$$

Since delta kernels are singular, they cannot be defined continuously in computer. Sequences of approximations T_α can be constructed such that T_α converge to T in order to smooth the singularity:

$$\lim_{\alpha \to \alpha_0} T_\alpha(x) \to T(x), \tag{3}$$

where α_0 is a generalized limit. Therefore, a DSC can be determined as:

$$F_\alpha(x) = \sum_k T_\alpha(x - x_k) f(x_k). \tag{4}$$

Here, $F_\alpha(x)$ is an approximation to $F(x)$ and $\{x_k\}$ is an approximate set of discrete points. $f(x)$ is a function replacing the original test function $\eta(x)$. A sequence of approximation can be improved by a regularizer. Gaussian regularizer is a typical delta regularizer and it is in the form of:

$$R_\sigma(x) = e^{-x^2/2\sigma^2} \tag{5}$$

where σ is the standard deviation. Shannon's delta kernel with sampling parameter a is in the following form:

$$T_\alpha = \frac{\sin \alpha x}{\pi x}. \tag{6}$$

In vibration analysis, a discretized form of Equation (6), which is sampled by Nyquist frequency ($a = \pi/\Delta$, Δ is the grid spacing) and improved by Gaussian regularizer, can be chosen as the kernel function of the DSC [12]:

$$\delta_{\pi/\Delta,\sigma}(x - x_k) = \frac{\sin[\pi/\Delta(x - x_k)]}{\pi/\Delta(x - x_k)} \exp\left(-(x - x_k)^2/2\sigma^2\right). \tag{7}$$

Here, Δ is determined by considering required precision of the analysis. The DSC expression can be rewritten by using regularized Shannon delta kernel (RSDK) given in Equation (7):

$$f(x) \approx \sum_{k=-\infty}^{\infty} \frac{\sin[\pi/\Delta(x - x_k)]}{\pi/\Delta(x - x_k)} \exp\left(-(x - x_k)^2/2\sigma^2\right) f(x_k). \tag{8}$$

As seen in Equation (8), since DSC approach is defined in an infinite region, the kernels must be bounded in a sufficient computational domain for numerical determination. This can be practically achieved by a spatial truncation of the convolution kernel.

A translationally invariant symmetric truncation algorithm can be used in an efficient bandwidth $(2M+1)$ as follows:

$$f^{(n)}(x_m) \approx \sum_{k=-M}^{M} \delta^{(n)}_{\pi/\Delta,\sigma}(x_m - x_k) f(x_k). \tag{9}$$

Here, x_m is the specific central point considered and $\delta^{(n)}_{\pi/\Delta,\sigma}(x)$ is the n-th derivative of $\delta(x)$ given in Equation (7) with respect to x.

DSC Implementation of Thin Composite Plates

Differential equation of harmonic bending vibration for a symmetrically laminated thin composite plate with natural frequency ω having side lengths a and b, total thickness h, average mass density ρ_0, and Poisson's ratio υ can be written in Cartesian co-ordinates (x, y) in terms of flexural displacement w as follows [30]:

$$\begin{aligned} D_{11}\frac{\partial^4 w(x,y)}{\partial x^4} + 4D_{16}\frac{\partial^4 w(x,y)}{\partial x^3 \partial y} + 2(D_{12}+2D_{66})\frac{\partial^4 w(x,y)}{\partial x^2 \partial y^2} \\ + 4D_{26}\frac{\partial^4 w(x,y)}{\partial x \partial y^3} + D_{22}\frac{\partial^4 w(x,y)}{\partial y^4} - \rho_0 h\omega^2 w(x,y) = 0. \end{aligned} \tag{10}$$

Here, D_{11}, D_{12}, D_{22}, D_{66} are the bending rigidities in the principle material directions whereas D_{16} and D_{26} are the bend-twist coupling stiffnesses. Introducing new nondimensional parameters: $X = x/a$, $Y = y/b$, $W = w/a$, $\lambda = a/b$, $D_\gamma = (D_{11}/D_{22})$, $D_\phi = (D_{12} + 2D_{66})/D_{22}$, $D_\alpha = (D_{16}/D_{22})$, $D_\beta = (D_{26}/D_{22})$, Equation (10) can be rewritten in the following form:

$$\begin{aligned} D_\gamma \frac{\partial^4 W(X,Y)}{\partial X^4} + 2\lambda^2 D_\phi \frac{\partial^4 W(X,Y)}{\partial X^2 \partial Y^2} + \lambda^4 \frac{\partial^4 W(X,Y)}{\partial Y^4} \\ + 4\left(\lambda D_\alpha \frac{\partial^4 W(X,Y)}{\partial X^3 \partial Y} + \lambda^3 D_\beta \frac{\partial^4 W(X,Y)}{\partial X \partial Y^3}\right) - \Omega^2 W(X,Y) = 0. \end{aligned} \tag{11}$$

Here Ω is the natural frequency parameter $(= \omega a^2\sqrt{\rho_0 h/D_{22}})$. Besides, for fully simply supported SOP; natural frequency parameter $\Omega_{p,q}$ is analytically given by [30]:

$$\Omega_{p,q} = \omega_{p,q}\, a^2 \sqrt{\frac{\rho_0 h}{D_{22}}} = \pi^2 \sqrt{p^4 D_\gamma + 2p^2 q^2 \lambda^2 D_\phi + q^4 \lambda^4} \quad p, q = 1, 2, 3, \ldots \tag{12}$$

Applying DSC approach in Equations (9)–(11) yields following eigenvalue equations for laminated composite plates together with applying DSC boundary condition implementation procedure [29]:

$$\begin{aligned} \Big\{ D_\gamma(\Gamma_x^{(4)} \otimes \mathrm{I}_y + 2\lambda^2 D_\phi(\Gamma_x^{(2)} \otimes \Gamma_y^{(2)}) + \lambda^4(\mathrm{I}_x \otimes \Gamma_y^{(4)}) \\ + 4\lambda\, D_\alpha(\Gamma_x^{(3)} \otimes \Gamma_y^{(1)}) + 4\lambda^3 D_\beta(\Gamma_x^{(1)} \otimes \Gamma_y^{(3)}) \Big\} \quad W = \Omega^2\, W. \end{aligned} \tag{13}$$

Here $W = \left\{ W_{0,0}, \ldots, W_{0,N-1}, W_{1,0}, \ldots, W_{1,N-1}, \ldots, \ldots, W_{N-1,0}, \ldots, W_{N-1,N-1} \right\}^T$ is nondimensional displacement vector and $\Gamma_y^{(n)}$ is a square DSC matrix as defined in ref. [29].

The DSC boundary condition implementation procedure assumes a relation between the bending displacements of auxiliary points and structure points as follows [19]

$$W(r_{-p}) - W(r_0) = A_{r,p}\big[W(r_p) - W(r_0)\big]. \quad p = 1, 2, \ldots, M(r = x \text{ or } y). \tag{14}$$

Equation (14) expresses that any auxiliary point can be written in terms of structure points. By taking into account the contribution of each auxiliary point to the bending displacement of structure points, the coefficient $A_{r,p}$ is found as -1 for simply supported and as $+1$ for clamped ends for each of p-values. A comprehensive verification study of DSC method for laminated composites can be found in ref. [29].

NUMERICAL APPLICATIONS

In this study, three different investigations labeled as Investigation A, B, and C were presented. General input parameters such as plate parameters and physical properties are tabulated in Table 1 for these studies. In all applications, linear vibration analyses were performed. The plates were assumed to be thin, square, and discretized by using $N = 21 \times 21$ grid points.

Table 1. General input parameters for three investigations.

General input parameters				
Investigation A				
Longitudinal modulus/ Transverse modulus	In-plane shear modulus/ Transverse modulus	Major Poisson's ratio (υ_{12})	Minor Poisson's ratio (υ_{21})	
$E_1/E_2 = 2.45$	$G_{12}/E_2 = 0.48$	$\upsilon_{12} = 0.23$	$\upsilon_{21} = 0.0939$	
Investigation B				
Properties	E-glass/ epoxy [31]	Kevlar/epoxy (Aramid 149/epoxy) [31]	Carbon/epoxy (AS4/3501-6) [31]	
Fiber volume ratio (V_f)	0.55	0.60	0.63	
Density (ρ, kg/m^3)	2100	1380	1580	
Longitudinal modulus (E_1, GPa)	39	87	142	
Transverse modulus (E_2, GPa)	8.6	5.5	10.3	
In-plane shear modulus (G_{12}, GPa)	3.8	2.2	7.2	
Major Poisson's ratio (υ_{12})	0.28	0.34	0.27	
Investigation C				
Properties	E-glass/ epoxy [31]	Kevlar/epoxy (Aramid 149/epoxy) [31]	Carbon/epoxy (AS4/3501-6) [31]	Aluminium alloy [10]
Fiber volume ratio (V_f)	0.55	0.60	0.63	–
Density (ρ, kg/m^3)	2100	1380	1580	–
Longitudinal modulus (E_1, GPa)	39	87	142	72.39
Transverse modulus (E_2, GPa)	8.6	5.5	10.3	72.39
In-plane shear modulus (G_{12}, GPa)	3.8	2.2	7.2	27.2
Major Poisson's ratio (υ_{12})	0.28	0.34	0.27	0.33

Investigation A: The Effects of Boundary Conditions, Orientation Angle, and Number of Plies on Natural Frequency Parameters of Thin Composite Plates

With six different boundary conditions and four different orientation angles, the DSC predictions of the first 10 natural frequency parameters of laminates with three, four, and five plies are tabulated in Tables 2–4, respectively. These tables also compare DSC frequency parameters with those of Chow et al.'s [2] work using Rayleigh–Ritz method and display very good agreement. The orientations of the stacks are considered as $(\theta, -\theta, \theta)$ for three-, $(\theta, -\theta, -\theta, \theta)$ for four-, and $(\theta, -\theta, \theta, -\theta, \theta)$ for five-ply laminates. Stacking sequences are labeled as P1 for $\theta = 0^\circ$, P2 for $\theta = 15^\circ$, P3 for $\theta = 30^\circ$, and P4 for $\theta = 45^\circ$. Boundary conditions are labeled as BC1, BC2,..., BC6 as presented in Tables 2–4. The natural frequency parameter $\beta = \omega a^2\sqrt{\rho_0 h/D_0}$ is determined by means of the rigidity $D_0 = E_1 h^3/(1 - \nu_{12}\nu_{21})$. Here a is the side length and h is the total thickness of the composite plate. ρ_0 is the average mass density, E_i, G_{ij}, and v_{ij} are elasticity modulus, shear modulus, and Poisson's ratio, respectively. Subscripts i and j denote principle fiber directions.

Figure 1 demonstrates the variation of the first natural mode with respect to number of lamination, boundary condition and stacking sequence. Figure 2 shows the variation of the tenth natural mode with respect to the same parameters. Figure 1 is an indicator of lower modes whereas Figure 2 reflects the feature of higher modes. The effects of number of plies and boundary condition are not clear for any of the stacking sequences in the lower modes. However, higher modes are rigorously affected by the change of number of plies and boundary condition when the orientation angle of the stacks is increased. In detail for higher modes, following inferences can be drawn with respect to four stacking sequences having different orientation angles:

- For P1: Number of plies and boundary condition do not influence frequencies.
- For P2: Number of plies (layers) seems to be effective on the frequency parameters regardless the type of boundary condition. Simply, increase in the number of layers increases the natural frequency parameters.
- For P3: Except BC4, the number of layers is quite effective for the other conditions.
- For P4: In this sequence, number of layers affects only plates with BC2, BC4, and BC5.

Investigation B: The Effects of Material, Boundary Condition, and Stacking Sequence on Free Vibration Characteristics of Polymer-based Thin Composite Plates

In this application, three different polymer materials with six stacking sequences and two boundary conditions are considered. Modal behaviors of composite plates with various combinations of these three main variables are examined. The examined boundary conditions are fully simply supported and fully clamped. In the analysis, stacking sequences are labeled as S1, S2,..., S6. These are,

- Symmetric cross ply (S1): $[0/90]_{2S}$
- Quasi-isotropic (S2): $[0/90/45/-45]_S$
- Symmetric angle ply (S3–S6): $[\theta/-\theta]_{2S}$

where $\theta = 15^\circ$, 30°, 45°, and 60° corresponding to stacking sequences S3, S4, S5, and S6, respectively. It is assumed that plates are composed of eight layers. In this analysis,

Table 2. Investigation A: natural frequency parameters of three-ply laminates (θ, $-\theta$, θ) with six different boundary conditions.

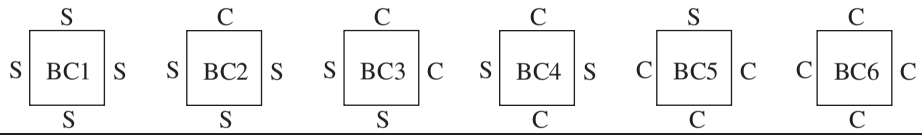

Three-ply Ply angle	Boundary condition	Mode sequence number									
		1	2	3	4	5	6	7	8	9	10
P1: (0°, 0°, 0°)	BC1 (Exact)	15.171	33.248	44.387	60.682	64.457	90.145	93.630	108.46	108.97	132.99
	BC1 (DSC)	15.171	33.248	44.387	60.682	64.457	90.145	93.630	108.46	108.97	132.99
	BC1 (Chow et al. [2])	15.19	33.31	44.52	60.78	64.55	90.31	93.69	108.7	–	–
	BC2 (DSC)	17.354	38.989	45.511	64.670	73.628	94.356	97.646	111.76	120.97	142.36
	BC3 (DSC)	21.398	41.419	55.176	72.474	75.276	103.68	109.26	122.20	125.22	148.83
	BC4 (DSC)	20.402	45.638	46.998	69.434	83.677	95.247	106.06	115.06	134.34	148.94
	BC5 (DSC)	27.007	44.856	66.216	77.465	81.733	110.94	123.75	125.49	140.12	154.50
	BC6 (DSC)	29.087	50.792	67.279	85.629	87.112	118.50	126.18	136.87	142.84	165.84
	BC6 (Chow et al. [2])	29.13	50.82	67.29	85.67	87.14	118.6	126.2	137.5	–	–
P2: (15°, −15°, 15°)	BC1 (DSC)	15.469	34.153	43.879	60.954	66.635	91.393	91.659	108.96	111.12	132.52
	BC1 (Chow et al. [2])	15.37	34.03	43.80	60.80	66.56	91.40	91.51	108.9	–	–
	BC2 (DSC)	17.707	39.813	45.192	65.290	75.599	92.211	98.975	112.30	123.59	140.57
	BC3 (DSC)	21.471	42.213	54.243	72.187	77.563	104.87	106.45	124.16	125.31	148.40
	BC4 (DSC)	20.791	45.514	47.739	70.200	85.623	93.210	106.82	116.38	137.04	148.24
	BC5 (DSC)	26.731	45.417	64.738	77.841	82.626	111.57	121.97	126.43	138.63	155.18
	BC6 (DSC)	28.897	51.405	65.911	84.515	89.712	119.21	122.74	139.30	141.93	165.24
	BC6 (Chow et al. [2])	28.92	51.43	65.92	84.55	89.76	119.3	122.7	139.9	–	–
P3: (30°, −30°, 30°)	BC1 (DSC)	16.058	36.060	42.743	61.757	71.849	85.780	94.096	109.23	119.25	133.47
	BC1 (Chow et al. [2])	15.86	35.77	42.48	61.27	71.41	85.67	93.60	108.9	–	–
	BC2 (DSC)	18.495	41.053	45.229	66.506	81.026	86.983	100.81	114.13	132.19	140.98
	BC3 (DSC)	21.629	44.109	52.052	72.280	82.937	99.361	106.91	123.28	133.61	148.77
	BC4 (DSC)	21.786	44.476	50.622	71.730	87.959	91.845	107.41	120.40	146.07	148.10
	BC5 (DSC)	26.046	46.935	61.041	78.224	86.059	113.03	113.03	132.74	137.05	156.28
	BC6 (DSC)	28.522	53.124	62.683	83.821	95.158	114.13	120.64	138.58	149.10	164.97
	BC6 (Chow et al. [2])	28.55	53.15	62.71	83.83	95.21	114.1	120.7	138.6	–	–

(Continued)

Table 2. Continued.

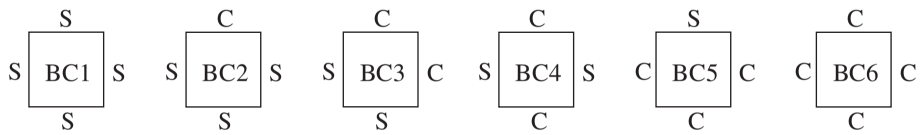

Three-ply Ply angle	Boundary condition	Mode sequence number									
		1	2	3	4	5	6	7	8	9	10
P4: (45°, −45°, 45°)	BC1 (DSC)	16.348	37.146	42.033	62.234	77.213	80.130	95.076	109.48	130.82	132.82
	BC1 (Chow et al. [2])	16.08	36.83	41.67	61.65	76.76	79.74	94.40	109.0	–	–
	BC2	19.214	40.331	47.506	67.279	80.153	89.555	101.05	116.67	133.04	141.37
	BC3	21.707	45.480	50.521	72.467	89.174	92.119	107.84	122.75	146.60	148.55
	BC4	23.059	43.047	54.979	72.655	82.688	101.21	106.97	125.16	134.84	148.71
	BC5	25.247	48.930	56.869	78.013	92.264	102.55	114.18	130.64	148.89	156.83
	BC6	28.337	54.623	60.430	83.658	101.94	105.60	121.41	137.29	163.18	165.04
	BC6 (Chow et al. [2])	28.38	54.65	60.45	83.65	102.0	105.6	121.4	137.3	–	–

Table 3. Investigation A: natural frequency parameters of four-ply laminates ($\theta, -\theta, -\theta, \theta$) with six different boundary conditions.

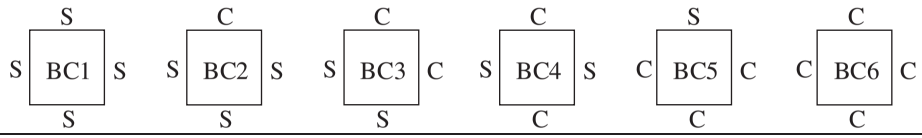

Four-ply Ply angle	Boundary condition	Mode sequence number									
		1	2	3	4	5	6	7	8	9	10
P1: (0°, 0°, 0°, 0°)	BC1 (Exact)	15.171	33.248	44.387	60.682	64.457	90.145	93.630	108.46	108.97	132.99
	BC1 (DSC)	15.171	33.248	44.387	60.682	64.457	90.145	93.630	108.46	108.97	132.99
	BC1 (Chow et al. [2])	15.19	33.31	44.52	60.78	64.55	90.31	93.69	108.7	–	–
	BC2 (DSC)	17.354	38.989	45.511	64.670	73.628	94.356	97.646	111.76	120.97	142.36
	BC3 (DSC)	21.398	41.419	55.176	72.474	75.276	103.68	109.26	122.20	125.22	148.83
	BC4 (DSC)	20.402	45.638	46.998	69.434	83.677	95.247	106.06	115.06	134.34	148.94
	BC5 (DSC)	27.007	44.856	66.216	77.465	81.733	110.94	123.75	125.49	140.12	154.50
	BC6 (DSC)	29.087	50.792	67.279	85.629	87.112	118.50	126.18	136.87	142.84	165.84
	BC6 (Chow et al. [2])	29.13	50.82	67.29	85.67	87.14	118.6	126.2	137.5	–	–
P2: (15°, −15°, −15°, 15°)	BC1 (DSC)	15.490	34.235	43.904	61.333	66.520	91.446	92.217	109.11	111.03	133.86
	BC1 (Chow et al. [2])	15.40	34.15	43.84	61.23	66.48	61.47	92.13	109.1	–	–
	BC2 (DSC)	17.731	39.934	45.186	65.615	75.559	92.259	99.620	112.33	123.57	141.99
	BC3 (DSC)	21.506	42.315	54.281	72.645	77.427	105.48	106.51	124.40	125.19	149.82
	BC4 (DSC)	20.817	45.790	47.588	70.517	85.617	93.250	107.64	116.25	137.04	149.59
	BC5 (DSC)	26.772	45.525	64.795	78.272	82.550	112.22	122.04	126.40	138.81	156.34
	BC6 (DSC)	28.940	51.528	65.959	85.070	89.530	119.88	122.82	139.41	141.96	166.70
	BC6 (Chow et al. [2])	28.98	51.56	65.97	85.11	89.57	119.9	122.8	140.1	–	–
P3: (30°, −30°, −30°, 30°)	BC1 (DSC)	16.117	36.426	42.696	62.764	71.737	85.828	96.009	109.47	119.07	136.76
	BC1 (Chow et al. [2])	15.94	36.23	42.52	62.46	71.45	85.79	95.71	109.3	–	–
	BC2 (DSC)	18.568	41.621	45.017	67.500	81.072	86.958	102.96	114.14	132.16	144.38
	BC3 (DSC)	21.730	44.521	52.062	73.413	82.855	99.451	108.97	123.64	133.46	152.29
	BC4 (DSC)	21.874	44.957	50.539	72.771	88.109	91.747	109.71	120.32	146.19	148.09
	BC5 (DSC)	26.164	47.306	61.152	79.525	85.867	113.24	114.99	133.53	136.67	159.79
	BC6 (DSC)	28.648	53.597	62.720	85.093	95.088	114.26	122.85	139.08	148.93	168.72
	BC6 (Chow et al. [2])	28.69	53.62	62.74	85.09	95.15	114.3	122.9	139.1	–	–

(Continued)

Table 3. Continued.

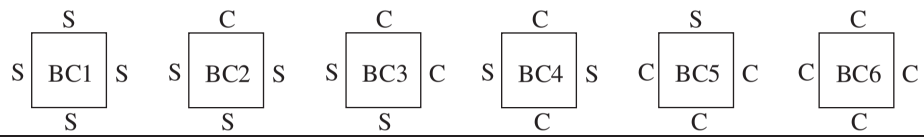

Four-ply Ply angle	Boundary condition	Mode sequence number									
		1	2	3	4	5	6	7	8	9	10
P4: (45°, −45°, −45°, 45°)	BC1 (DSC)	16.424	37.837	41.766	63.54	77.644	79.646	97.783	109.65	131.13	132.43
	BC1 (Chow et al. [2])	16.17	37.62	41.52	63.15	77.33	79.40	97.32	109.4	–	–
	BC2 (DSC)	19.316	40.909	47.419	68.692	80.174	89.503	103.80	117.00	132.94	145.76
	BC3 (DSC)	21.840	46.273	50.291	73.908	89.667	91.704	110.77	123.00	146.95	148.22
	BC4 (DSC)	23.190	43.540	55.058	74.218	82.562	101.30	109.67	125.91	134.51	153.18
	BC5 (DSC)	25.396	49.593	56.824	79.572	92.345	102.55	117.16	131.07	148.85	161.50
	BC6 (DSC)	28.503	55.534	60.197	85.254	102.52	105.18	124.59	137.64	163.64	165.32
	BC6 (Chow et al. [2])	28.53	55.56	60.22	85.25	102.6	105.2	124.5	137.6	–	–

Table 4. Investigation A: natural frequency parameters of five-ply laminates ($\theta, -\theta, \theta, -\theta, \theta$) with six different boundary conditions.

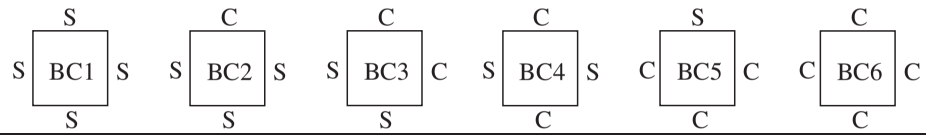

Five-ply Ply angle	Boundary condition	Mode sequence number									
		1	2	3	4	5	6	7	8	9	10
P1: (0°, 0°, 0°, 0°,0°)	BC1 (Exact)	15.171	33.248	44.387	60.682	64.457	90.145	93.630	108.46	108.97	132.99
	BC1 (DSC)	15.171	33.248	44.387	60.682	64.457	90.145	93.630	108.46	108.97	132.99
	BC1 (Chow et al. [2])	15.19	33.31	44.52	60.78	64.55	90.31	93.69	108.7	–	–
	BC2 (DSC)	17.354	38.989	45.511	64.670	73.628	94.356	97.646	111.76	120.97	142.36
	BC3 (DSC)	21.398	41.419	55.176	72.474	75.276	103.68	109.26	122.20	125.22	148.83
	BC4 (DSC)	20.402	45.638	46.998	69.434	83.677	95.247	106.06	115.06	134.34	148.94
	BC5 (DSC)	27.007	44.856	66.216	77.465	81.733	110.94	123.75	125.49	140.12	154.50
	BC6 (DSC)	29.087	50.792	67.279	85.629	87.112	118.50	126.18	136.87	142.84	165.84
	BC6 (Chow et al. [2])	29.13	50.82	67.29	85.67	87.14	118.6	126.2	137.5	–	–
P2: (15°, −15°, 15°, −15°, 15°)	BC1 (DSC)	15.506	34.296	43.922	61.630	66.419	91.485	92.642	109.21	110.98	135.01
	BC1 (Chow et al. [2])	15.46	34.24	43.88	61.59	66.42	91.52	92.62	109.3	–	–
	BC2 (DSC)	17.749	40.026	45.180	65.861	75.526	92.295	100.12	112.33	123.56	143.21
	BC3 (DSC)	21.533	42.391	54.310	73.009	77.303	105.94	106.56	124.57	125.11	151.00
	BC4 (DSC)	20.837	46.036	47.436	70.757	85.610	93.280	108.29	116.11	137.04	150.69
	BC5 (DSC)	26.803	45.605	64.837	78.613	82.472	112.71	122.10	126.36	138.95	157.25
	BC6 (DSC)	28.972	51.620	65.995	85.527	89.350	120.40	122.87	139.48	142.00	167.91
	BC6 (Chow et al. [2])	29.00	51.65	66.01	85.55	89.40	120.5	122.9	140.1	–	–
P3: (30°, −30°, 30°, −30°, 30°)	BC1 (DSC)	16.161	36.705	42.652	63.561	71.598	85.864	97.550	109.52	118.94	139.55
	BC1 (Chow et al. [2])	15.98	36.58	42.53	63.37	71.43	85.86	97.42	109.4	–	–
	BC2 (DSC)	18.622	42.109	44.792	68.264	81.065	86.946	104.75	113.93	132.12	147.17
	BC3 (DSC)	21.806	44.830	52.065	74.303	82.738	99.517	110.61	123.79	133.35	155.27
	BC4 (DSC)	21.939	45.330	50.459	73.569	88.172	91.688	111.68	120.00	146.26	148.10
	BC5 (DSC)	26.251	47.580	61.232	80.620	85.587	113.34	116.58	134.07	136.34	162.73
	BC6 (DSC)	28.740	53.951	62.741	86.097	94.968	114.35	124.61	139.33	148.80	171.89
	BC6 (Chow et al. [2])	28.78	53.98	62.76	86.09	95.04	114.4	124.6	139.3	–	–

(Continued)

Table 4. Investigation A: natural frequency parameters of five-ply laminates ($\theta, -\theta, \theta, -\theta, \theta$) with six different boundary conditions.

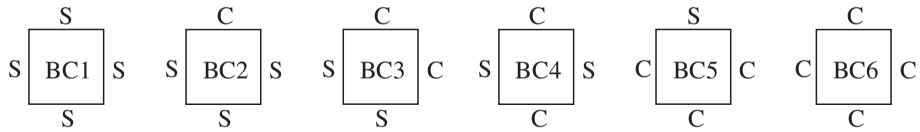

Five-ply Ply angle	Boundary condition	Mode sequence number									
		1	2	3	4	5	6	7	8	9	10
P4: (45°, −45°, 45°, −45°, 45°)	BC1 (DSC)	16.480	38.436	41.478	64.563	77.958	79.223	100.09	109.47	131.32	132.14
	BC1 (Chow et al. [2])	16.29	38.30	41.32	64.35	77.77	79.09	99.79	109.3	–	–
	BC2 (DSC)	19.391	41.354	47.333	69.808	80.102	89.468	106.09	116.98	132.85	146.63
	BC3 (DSC)	21.940	46.954	50.024	75.025	90.027	91.337	113.26	122.86	147.20	147.98
	BC4 (DSC)	23.286	43.905	55.110	75.506	82.324	101.37	111.85	126.28	134.24	156.97
	BC5 (DSC)	25.504	50.101	56.768	80.794	92.317	102.55	119.62	131.11	148.79	163.48
	BC6 (DSC)	28.624	56.308	59.917	86.486	102.95	104.81	127.27	137.56	163.95	165.06
	BC6 (Chow et al. [2])	28.68	56.34	59.94	86.48	103.0	104.9	127.3	137.5	–	–

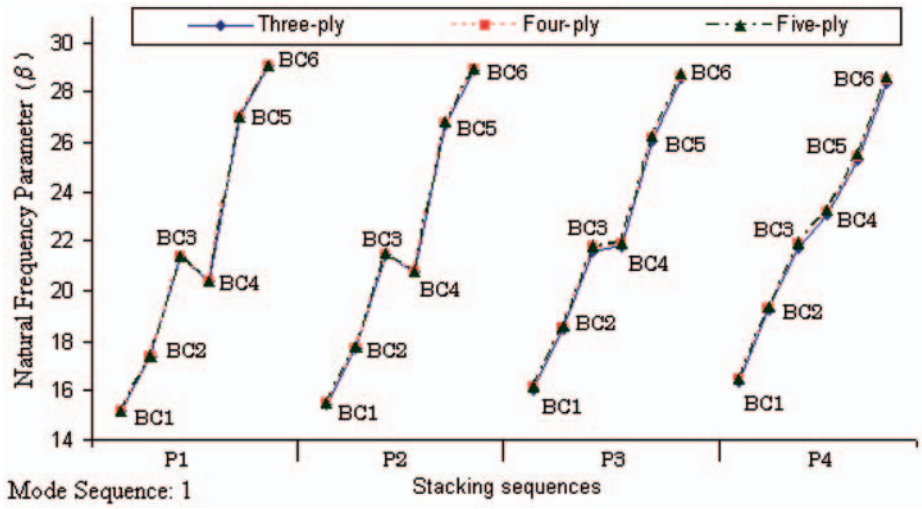

Figure 1. *Investigation A: natural frequency parameters of composite plates with respect to number of lamination, boundary condition, and stacking sequence for mode sequence 1.*

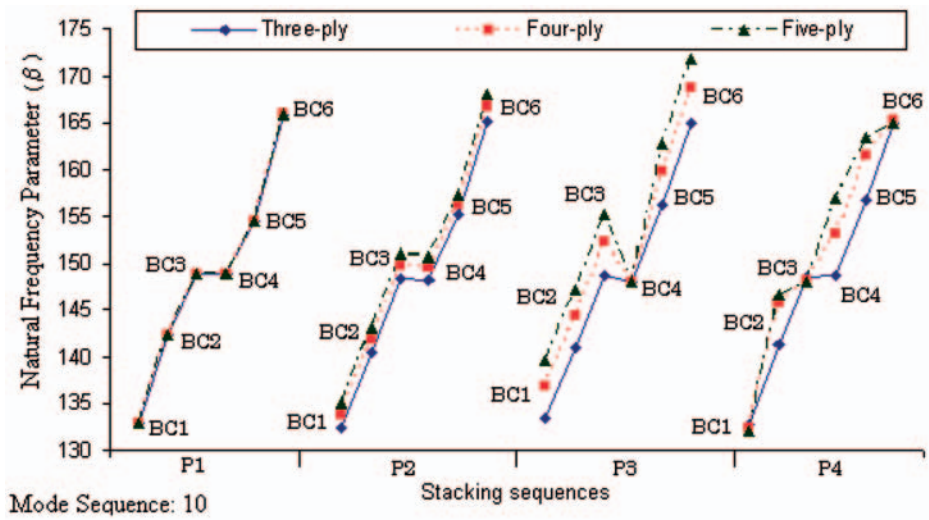

Figure 2. *Investigation A: natural frequency parameters of composite plates with respect to number of lamination, boundary condition, and stacking sequence for mode sequence 10.*

the natural frequency parameter is defined as $\Omega/\pi^2 = \omega a^2\sqrt{\rho_0 h/D_{22}}$ for numerical facility. Here D_{22} is the bending rigidity in a principle direction.

Generally, prediction of nondimensional natural frequency parameters is sufficient for parametric free vibration analysis. Because, in most parametric cases, there is a definite simple relation between frequency parameters and natural frequencies. However, since variables representing material and stack are embedded in vibration equations; the relation between natural frequencies and these variables is implicit. For this reason, computation

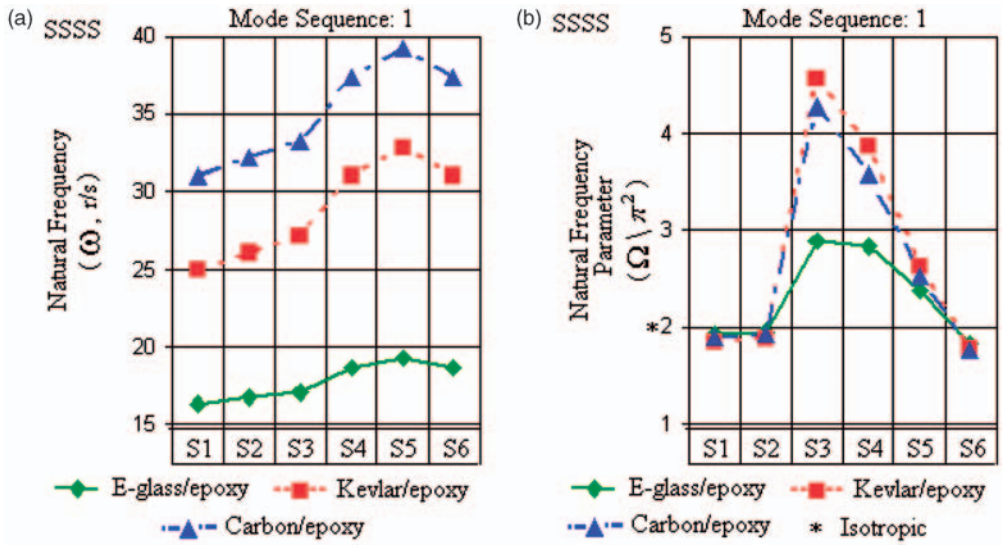

Figure 3. *Investigation B: (a) natural frequencies, (b) natural frequency parameters of simply supported composite plates with several stacking sequences for mode sequence 1.*

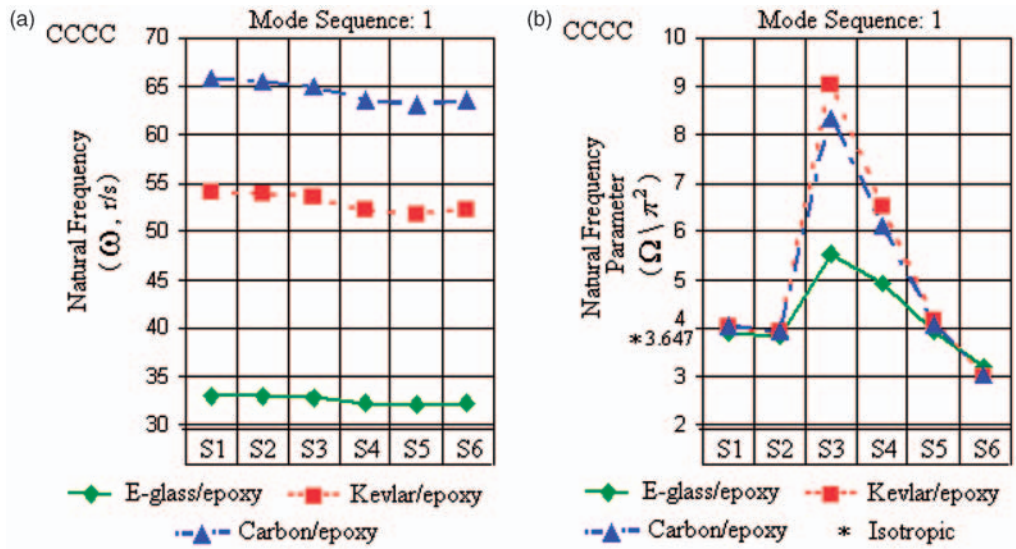

Figure 4. *Investigation B: (a) natural frequencies, (b) natural frequency parameters of clamped composite plates with several stacking sequences for mode sequence 1.*

of natural frequencies beside natural frequency parameters would be meaningful in order to examine special modal features of composite plates made of different materials and stacking sequences, as performed in this analysis.

Figures 3(a) and –8(a) display natural frequencies whereas Figures 3(b) and –8(b) show frequency parameters of the plates for mode sequences 1, 2, and 10, respectively.

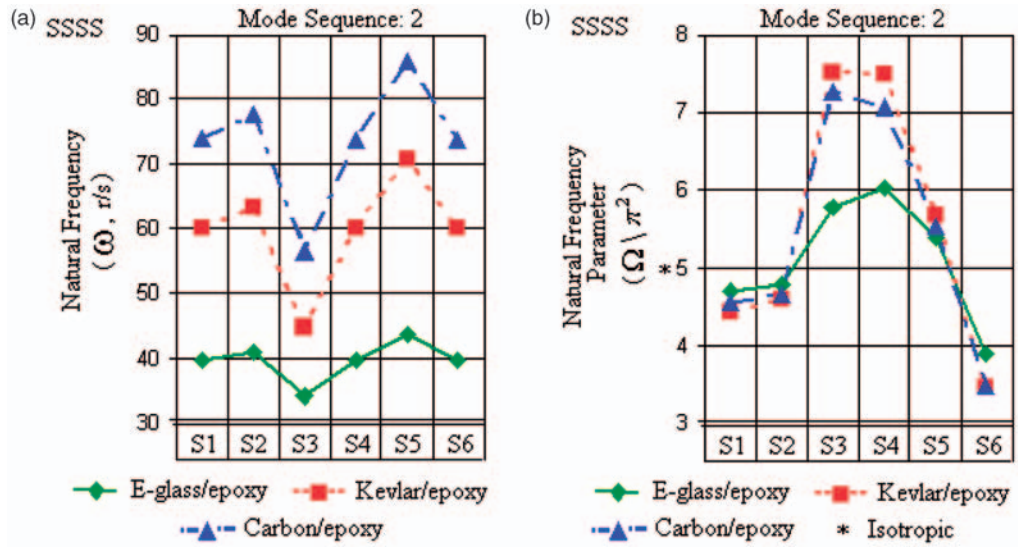

Figure 5. *Investigation B: (a) natural frequencies, (b) natural frequency parameters of simply supported composite plates with several stacking sequences for mode sequence 2.*

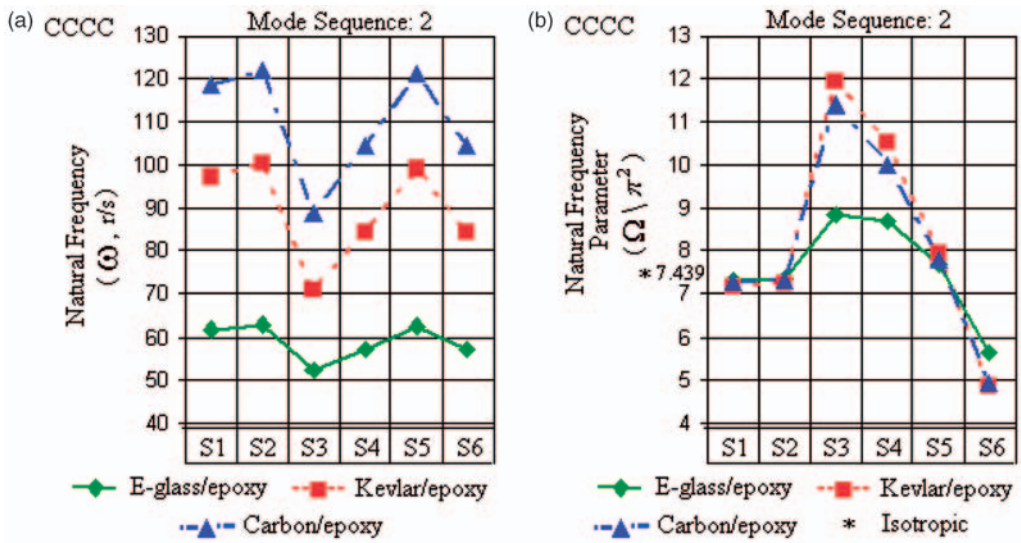

Figure 6. *Investigation B: (a) natural frequencies, (b) natural frequency parameters of clamped composite plates with several stacking sequences for mode sequence 2.*

Since similar variation trends for frequencies are observed in Figures 3–8, these modal features may be generalized to the other modes. Table 5 displays the first 20 mode shapes of an isotropic plate and compares them with the similar first 10 mode shapes of composite plates. Table 6 presents nondimensional bending and bend-twist rigidity values, which may give useful information for the examination of modal characteristics in detail.

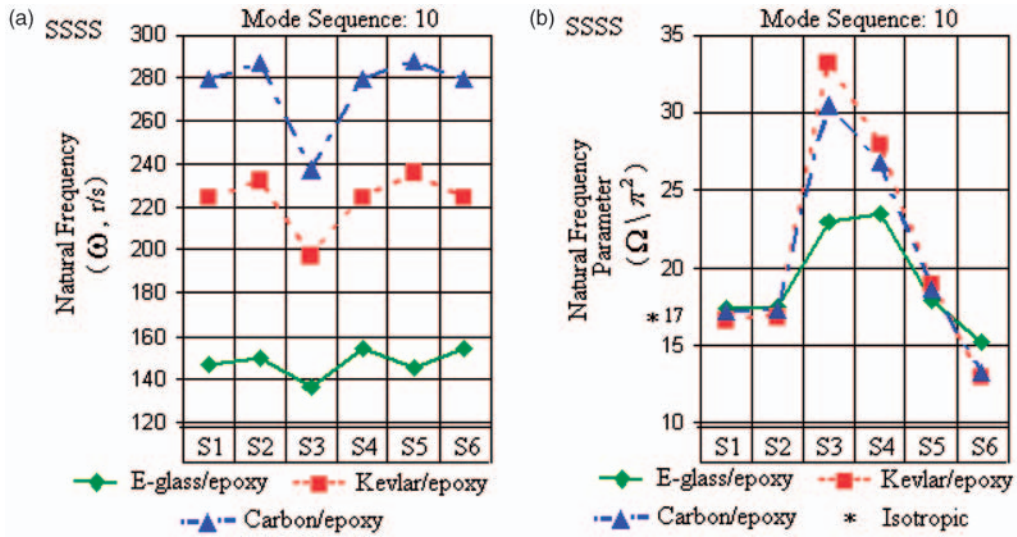

Figure 7. *Investigation B: (a) natural frequencies, (b) natural frequency parameters of simply supported composite plates with several stacking sequences for mode sequence 10.*

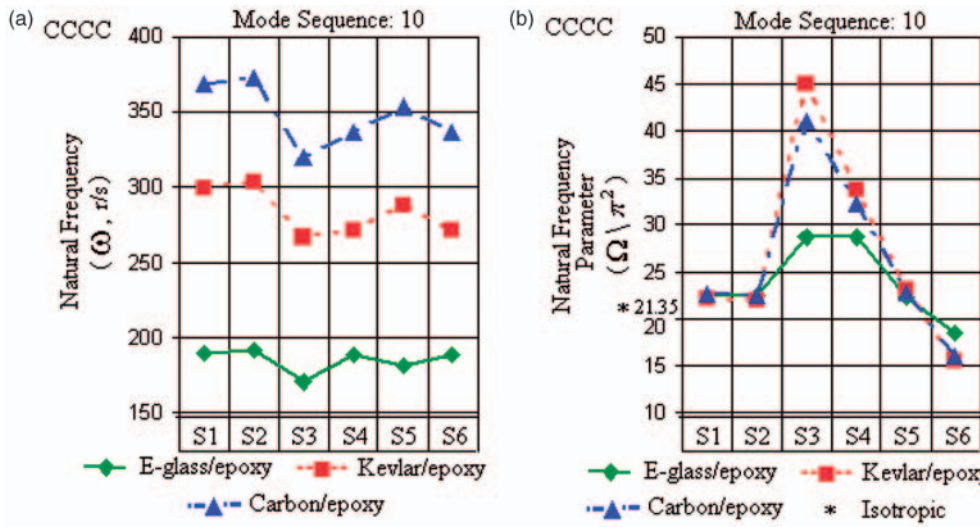

Figure 8. *Investigation B: (a) natural frequencies, (b) natural frequency parameters of clamped composite plates with several stacking sequences for mode sequence 10.*

When Figures 3–8 and Tables 5 and 6 are examined together the following conclusions can be drawn:

- The variation of natural frequencies with respect to stacking sequences is very similar for the three composites for a specific boundary condition.
  – Natural frequencies of the plates made of all three materials are not considerably affected by selecting S1 or S2 stacking sequences. This is due to the fact that materials with S1 and S2 have nondimensional plate rigidities D_γ and D_ϕ in the same order

Table 5. Investigation B: isotropic plate bending mode shapes (1–20) and corresponding laminated composite plate bending mode sequences (1–10).

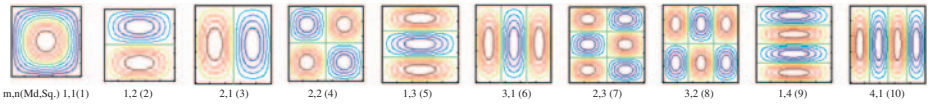

St. sq.	Material: E-glass/epoxy composite (mode sequences: 1–10)									
S1–S2	1	2	3	4	5	6	7	8	9	–
S3	1	2	3	5	4	8	6	9	7	–
S4	1	2	3	5	4	6	7	9	8	–
S5	1	2	3	4	5	6	7	8	9	10
S6	1	3	2	5	6	4	8	7	–	8
St. sq.	Material: Kevlar/epoxy and carbon/epoxy composites (mode sequences: 1–10)									
S1–S2	1	2	3	4	5	7	6	8	9	–
S3	1	2	4	5	3	10	7	–	6	–
S4	1	2	3	5	4	7	8	9	6	–
S5	1	2	3	4	5	6	7	8	9	10
S6	1	3	2	5	7	4	9	8	–	6

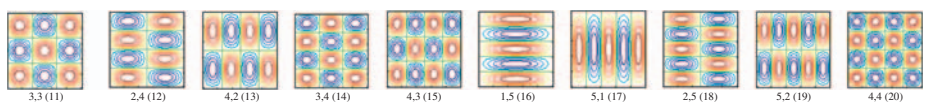

St. sq.	Material: E-glass/epoxy composite (mode sequences: 1–10)									
S1–S2	10	–	–	–	–	–	–	–	–	–
S3	–	10	–	–	–	–	–	–	–	–
S4	–	10	–	–	–	–	–	–	–	–
S5	–	–	–	–	–	–	–	–	–	–
S6	–	–	10	–	–	–	–	–	–	–
St. sq.	Material: Kevlar/epoxy and Carbon/epoxy composites (mode sequences: 1–10)									
S1–S2	10	–	–	–	–	–	–	–	–	–
S3	–	9	–	–	–	8	–	–	–	–
S4	–	–	–	–	–	10	–	–	–	–
S5	–	–	–	–	–	–	–	–	–	–
S6	–	–	–	–	–	–	10	–	–	–

of magnitude. On the contrary, symmetric angle-ply sequences drastically influence natural frequencies depending on the orientation angle (Figures 3(a) and –8(a), Table 6).
– The same natural frequencies are obtained for S4 and S6 due to the fact that their orientation angles are complementary angles of each others (Figures 3(a) and –(8a)).
– Apparently, the plate made of carbon/epoxy has the highest natural frequencies and therefore is determined as the most rigid one. Kevlar/epoxy is less rigid and evidently the most elastic one is E-glass/epoxy (Figures 3(a) and 8(a)). This property also may be inspected from Table 6 as E-glass/epoxy having generally the lowest nondimensional rigidities.

- The change of boundary condition highly affects natural frequency-stacking sequence relation especially in the first mode, which is the most boundary condition-dependent mode (Figures 3(a) and 8(a)).
  – The first natural frequencies of angle-plied plates (S3–S6) are higher than those of S1 and S2 plates for SSSS and vice versa for CCCC conditions. It may be stated that the change of boundary condition completely reverses the variation trend of the first

Table 6. Investigation B: nondimensional bending rigidities (D_γ, D_ϕ) and bend-twist coupling rigidities (D_α, D_β) of composite plates consisting of eight layers with different material properties and stacking sequences.

Stacking Sequences	E-glass/epoxy				Kevlar/epoxy				Carbon/epoxy			
	D_γ	D_ϕ	D_α	D_β	D_γ	D_ϕ	D_α	D_β	D_γ	D_ϕ	D_α	D_β
Symmetric cross ply (S1)	1.6298	0.5457	0	0	1.9869	0.2014	0	0	1.9598	0.3324	0	0
Quasi isotropic (S2)	1.4583	0.6694	0.0382	0.0382	1.7099	0.4255	0.0592	0.0592	1.6867	0.5224	0.0572	0.0572
Symmetric angle ply												
15° (S3)	3.9594	1.6972	0.2873	0.0331	12.8470	3.5654	1.1865	0.0960	10.7140	3.3425	0.9341	0.1175
30° (S4)	2.3845	2.3264	0.3278	0.1219	4.7487	4.7148	0.9076	0.3099	4.1234	3.9620	0.7346	0.2798
45° (S5)	1.0000	1.8269	0.1693	0.1693	1.0000	2.5246	0.2911	0.2911	1.0000	2.2663	0.2648	0.2648
60° S6)	0.4194	0.9756	0.0511	0.1375	0.2106	0.9929	0.0653	0.1911	0.2425	0.9609	0.0679	0.1781
Isotropic	1.0000	1.0000	0	0								

natural frequency with respect to S1–S6 sequences.

– S5 plate made of carbon/epoxy is the most rigid plate among simply supported plates (Figures 3(a), 5(a), and 7(a)) whereas S2 plate made of carbon/epoxy is the most rigid one among the clamped plates (Figures 4(a), 6(a), and 8(a)). In particular, the plate with S2-carbon/epoxy-clamped combination has the highest natural frequencies.

- Mode shapes clearly show that some modal replacements are encountered in composite plates, generally, after the first two modes.

  – Considerable mode shape replacements with isotropic plates are observed in particular for angle ply sequences (except S5) compared to S1 and S2 sequences (Table 5). This is because S1 and S2 sequences have comparatively close rigidities to isotropic plates (Table 6).

  – Stack S5 shows resembling modal characteristics to isotropic plates since it has equal rigidities in both directions ($D_\gamma = 1$) (Tables 5 and 6).

  – Having close D_γ and D_ϕ values, stacks S1 and S2 have the same mode shapes and are shown together (Tables 5 and 6).

  – Having complementary orientation angles, stacks S4 and S6 show inverse nodal lines with respect to each other except for diagonally symmetric mode shapes (Table 5).

  – The same mode shapes are obtained for carbon/epoxy and Kevlar/epoxy and they are shown together in Table 5. These two materials have similar rigidities as shown in Table 6. Natural frequencies are affected by small differences in variables but mode shapes are not.

  – For these materials and orientations, boundary conditions do not considerably affect the mode shapes and thus, similar shapes are obtained for SSSS and CCCC conditions (Table 5).

  – There is almost an explicit relation between mode shapes in Table 5 and nondimensional rigidities in Table 6. For instance, $D_\gamma \neq 1$ implies that the rigidity of the plate in a direction is higher than the other one. The other nondimensional rigidities D_ϕ, D_α, and D_β reflect a coupling behavior between the two directions. This coupling leads to small shape changes compared to isotropic plate; however, these small differences are not considerable in such a general analysis.

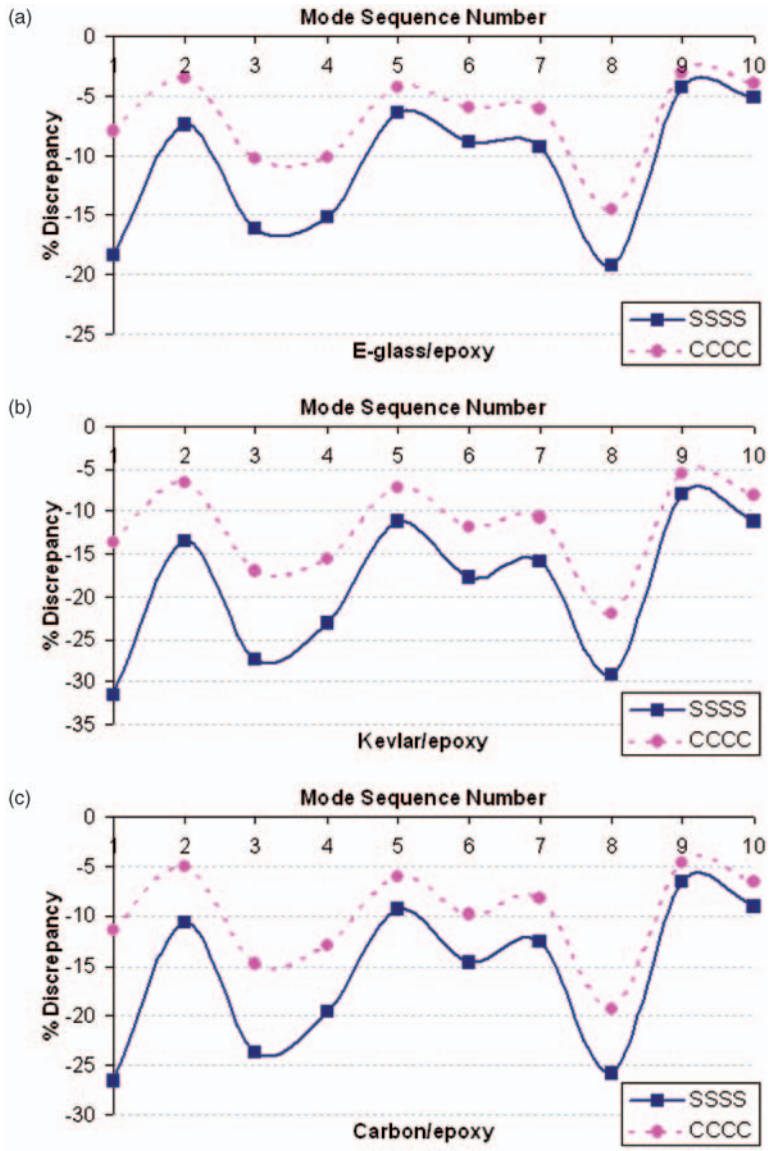

Figure 9. *Investigation B: discrepancies of natural frequency parameters of composite plates with S5 sequence made of (a) E-glass/epoxy; (b) Kevlar/epoxy; (c) carbon/epoxy materials, from an isotropic plate.*

- Stacking sequences considerably change the deviation of a composite plate from an isotropic plate (Figures 3(b) and (8b)).
  – Plates with S1 and S2 sequences approximately have the same frequency parameters with an isotropic plate (Figures 3(b) and –(8b)).
  – In the angle plies, S3 and S4 have higher positive deviations from isotropic plate. S5 is the least deviated angle ply, whereas S6 negatively deviates.
  – Frequency parameters of plates with 45° orientation angle (S5) are very close to that of an isotropic plate (Figures 3(b) and –8(b)). The discrepancy for CCCC plates is less,

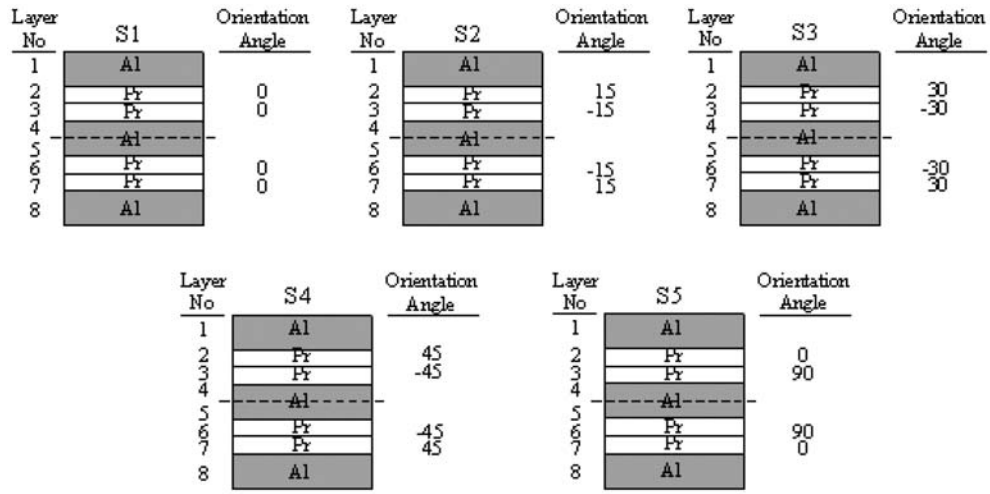

Figure 10. *Investigation C: schematic representation of five different stacking sequences of FML composite plates (Al.: aluminium, Pr.: prepregs).*

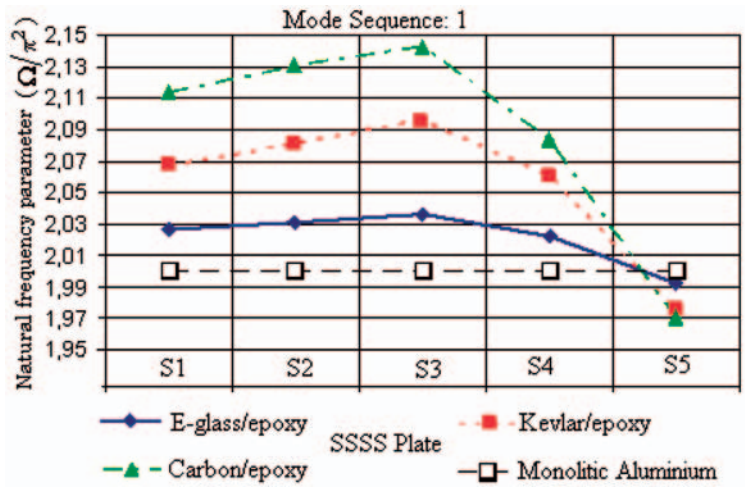

Figure 11. *Investigation C: natural frequency parameters of simply supported FML composite plates with several stacking sequences for mode sequence 1.*

as obviously seen from the modal spectra in Figure 9. This phenomenon implies that increase of the rigidity with CCCC condition exposes uniform modal characteristics as suppressing prominent features of composite materials.

Investigation C: The Effects of Material, Boundary Condition, and Orientation Angle on Natural Frequency Parameters of FML Plates

Natural frequency parameters of aluminium/E-glass-epoxy, aluminium/Kevlar-epoxy, and aluminium/carbon-epoxy plates with five stacking sequences shown in Figure 10

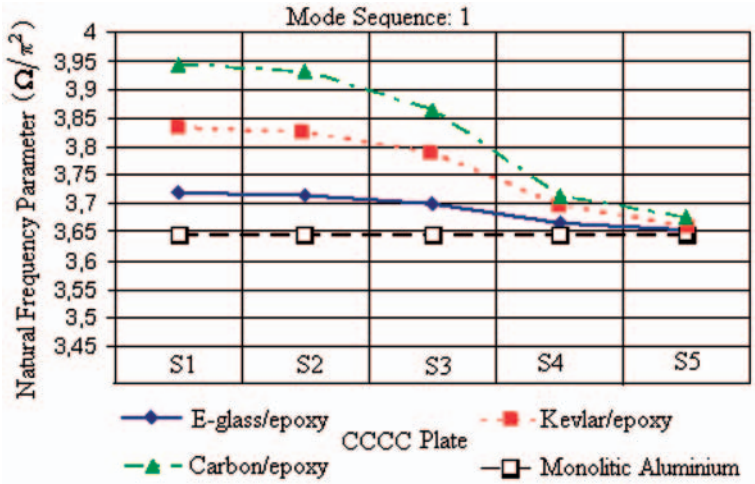

Figure 12. *Investigation C: natural frequency parameters of clamped FML composite plates with several stacking sequences for mode sequence 1.*

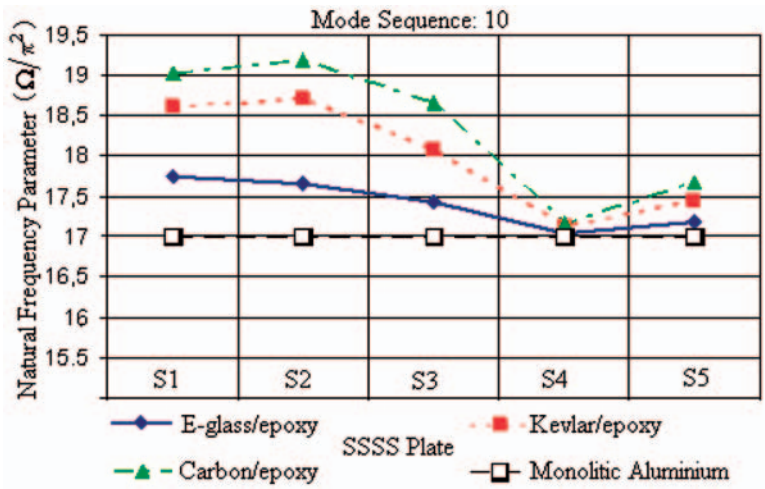

Figure 13. *Investigation C: natural frequency parameters of simply supported FML composite plates with several stacking sequences for mode sequence 10.*

were obtained in this application. Figures 11–14 exhibit the effects of material, boundary condition, and fiber orientation on natural frequency parameters. Figures 11 and 12 for Mode 1 generally reflect the characteristics of the first few modes whereas Figures 13 and 14 for Mode 10 reflect the feature of higher modes. The following observations may be made from Figures 11–14:

- For the first few modes of all polymer prepregs, S3 plates with simply supported and S1 plates with clamped boundary conditions have higher frequency parameters. However, for higher modes, stacks having small orientation angles (S1,S2) provide higher frequency parameters independent of the boundary conditions.

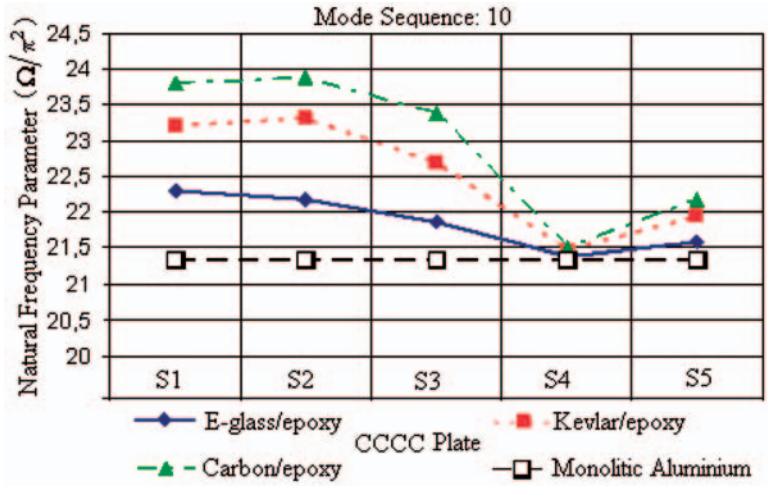

Figure 14. *Investigation C: natural frequency parameters of clamped FML composite plates with several stacking sequences for mode sequence 10.*

- Frequency parameters of S4 plates seem to be very close to those of monolithic aluminium alloy plates, except for the first few modes of simply supported plates shown in Figure 11. This similarity is mostly encountered at higher modes where boundary conditions lose their effect.
- In general, aluminium/polymer prepregs have higher frequency parameters compared to monolithic aluminium alloys.
- In general aluminium/carbon-epoxy plates have higher frequency parameters than the other FMLs.
- The exception to the previous two observations is variation of S5. This stack triggers different modal tendencies from the others. Therefore, S5 should be exclusively taken into consideration in engineering design.

CONCLUSIONS

For the elimination of unwanted vibration and sound for a product, modal behaviors of structural elements such as beams, plates, and acoustic enclosures forming the entire body must be primarily determined in the design stage by using experimental or computational techniques. With the substitution of composite materials for plastic and metal materials due to their high quality mechanical properties, researchers have been increasingly dealing with the dynamic analysis of structural elements made of various polymer and/or polymer–metal materials. In this regard, present study is mainly devoted to the vibrational behavior of various thin composite plates.

In this study, various composite plates of practical importance were considered on the basis of three free vibration applications. The DSC, a recent approach, was successfully used as a computational technique. Effects of material type and orientation angle along with boundary conditions on the modal characteristics of various symmetrically laminated composite plates were examined in detail. Investigation A revealed that higher modes are

affected considerably by number of plies and boundary conditions, especially when the orientation angle of the stacks is increased. Investigation B mainly proved that the type of fiber material and stacking sequence rigorously change the modal features of the laminates and simply cause modal replacements. Investigation C exposed that the stack orientated by 0°–90° ply angles show different modal tendencies from the other stacks. As a consequence, material and sequence type with the orientation angle should be selected expediently for the design objectives by considering the type of boundary conditions and frequency range of operation.

REFERENCES

1. Leissa, A.W. and Narita, Y. (1989). Vibration Studies for Simply Supported Symmetrically Laminated Rectangular Plates, *Composite Structures*, **12**: 113–132.
2. Chow, S.T., Liew, K.M. and Lam, K.Y. (1992). Transverse Vibration of Symmetrically Laminated Rectangular Composite Plates, *Composite Structures*, **20**(4): 213–226.
3. Hung, K.C., Liew, K.M., Lim, K.M. and Leong, S.L. (1993). Boundary Beam Characteristics Orthonormal Polynomials in Energy Approach for Vibration of Symmetric Laminates-I: Classical Boundary Conditions, *Composite Structures*, **26**: 167–184.
4. Asundi, A. and Choi, A.Y.N. (1997). Fiber Metal Laminates: An Advanced Material for Future Aircraft, *Journal of Materials Processing Technology*, **63**: 384–394.
5. Vogelesang, L.B. and Vlot, A. (2000). Development of Fiber Metal Laminates for Advanced Aerospace Structures, *Journal of Materials Processing Technology*, **103**: 1–5.
6. Vermeeren, C.A.J.R. (2003). An Historic Overview of the Development of Fiber Metal Laminates, *Applied Composite Materials*, **10**: 189–205.
7. Botelho, E.C., Silva, R.A., Pardini, L.C. and Rezende, M.C. (2006). A Review on the Development and Properties of Continuous Fiber/Epoxy/Aluminium Hybrid Composites for Aircraft Structures, *Materials Research*, **9**: 247–256.
8. Barai, A. and Durvasula, S. (1992). Vibration and Buckling of Hybrid Laminated Curved Panels, *Composite Structures*, **21**(1): 15–27.
9. Lee, Y.S. and Kim, Y.W. (1996). Analysis of Nonlinear Vibration of Hybrid Composite Plates, *Computers and Structures*, **61**(3): 573–578.
10. Harras, B., Benamar, R. and White, R.G. (2002). Experimental and Theoretical Investigation of the Linear and Non-linear Dynamic Behaviour of a Glare 3 Hybrid Composite Panel, *Journal of Sound and Vibration*, **252**(2): 281–315.
11. Chen, C.S. (2005). Investigation on the Vibration and Stability of Hybrid Composite Plates, *Journal of Reinforced Plastics and Composites*, **24**(16): 1747–1758.
12. Wei, G.W. (1999). Discrete Singular Convolution for the Solution of Fokker-Plank Equation, *Journal of Chemical Physics*, **110**(18): 8930–8942.
13. Wei, G.W. (2000). Discrete Singular Convolution for the Sine-Gordon Equation, *Physica D*, **137**: 247–259.
14. Wei, G.W. (2000). Wavelets Generated by Using Discrete Singular Convolution, *Journal of Physics A*, **33**: 8577–8596.
15. Wei, G.W. (2001). Discrete Singular Convolution for Beam Analysis, *Engineering Structures*, **23**: 1045–1053.
16. Wei, G.W. (2001). Vibration Analysis by Using Discrete Singular Convolution, *Journal of Sound and Vibration*, **244**(3): 535–553.
17. Wei, G.W. (2001). A New Algorithm for Solving Some Mechanical Problems, *Computational Methods in Applied Mechanics and Engineering*, **190**: 2017–2030.
18. Wei, G.W., Zhao, Y.B. and Xiang, Y. (2001). The Determination of Natural Frequencies of Rectangular Plates with Mixed Boundary Conditions by Discrete Singular Convolution, *International Journal of Mechanical Sciences*, **43**: 1731–1746.

19. Wei, G.W., Zhao, Y.B. and Xiang, Y. (2002). Discrete Singular Convolution and its Application to the Analysis of Plates with Internal Supports. Part 1: Theory and Algorithm, *International Journal of Numerical Methods in Engineering*, **55**: 913–946.
20. Xiang, Y., Zhao, Y.B. and Wei, G.W. (2002). Discrete Singular Convolution and its Application to the Analysis of Plates with Internal Supports. Part 2: Applications, *International Journal of Numerical Methods in Engineering*, **55**: 947–971.
21. Zhao, Y.B., Wei, G.W. and Xiang, Y. (2002). Plate Vibrations under Irregular Internal Supports, *International Journal of Solids and Structures*, **39**: 1361–1383.
22. Zhao, Y.B. and Wei, G.W. (2002). DSC Analysis of Rectangular Plates with Non-uniform Boundary Conditions, *Journal of Sound and Vibration*, **255**(2): 203–228.
23. Zhao, Y.B., Wei, G.W. and Xiang, Y. (2005). DSC Analysis of Free-edged Beams by an Iteratively Matched Boundary Method, *Journal of Sound and Vibration*, **284**: 487–493.
24. Hou, Y., Wei, G.W. and Xiang, Y. (2005). DSC-Ritz Method for the Free Vibration Analysis of Mindlin Plates, *International Journal for Numerical Methods in Engineering*, **62**: 262–288.
25. Civalek, Ö. (2007). Numerical Analysis of Free Vibrations of Laminated Composite Conical and Cylindrical Shells: Discrete Singular Convolution (DSC) Approach, *Journal of Computational and Applied Mathematics*, **205**: 251–271.
26. Civalek, Ö. (2007). Free Vibration and Buckling Analyses of Composite Plates with Straight-sided Quadrilateral Domain Based on DSC Approach, *Finite Elements in Analysis and Design*, **43**(13): 1013–1022.
27. Civalek, Ö. (2007). A Parametric Study of the Free Vibration Analysis of Rotating Laminated Cylindrical Shells Using the Method of Discrete Singular Convolution, *Thin Walled Structures*, **45**: 692–698.
28. Seçgin, A., Atas, C. and Sarıgül, A.S. (2007). Investigation of the Effects of Material and Fiber Orientation Angles on the Modal Characteristics of Thin FML Composite Plates by Using Discrete Singular Convolution (DSC) Approach, In: *4th Ankara International Aerospace Conference,* Ankara, 10–12 September, Article No: AIAC-2007-045.
29. Seçgin, A. and Sarıgül, A.S. (2008). Free Vibration Analysis of Symmetrically Laminated Thin Composite Plates by Using Discrete Singular Convolution (DSC) Approach: Algorithm and Verification, *Journal of Sound and Vibration*, **315**: 197–211.
30. Whitney, J.M. (1987). *Structural Analysis of Laminated Anisotropic Plates*, Technomic Publishing Company Inc., Pennsylvania.
31. Daniel, I.M. and Ishai, O. (1994). *Engineering Mechanics of Composite Materials*, Oxford University Press, New York.